ISSN:1984-2295

Revista Brasileira de Geografia Física

Homepage:https://periodicos.ufpe.br/revistas/rbgfe

Soil Erosion Assessment Using RUSLE Model and GIS in Juma Watershed, Southern Amazonas State

Miqueias Lima Duarte[1], Eliomar Pereira da Silva Filho[2], Heron Salazar Costa[3] Tatiana Acácio da Silva[4]

[1]Doutorando em Ciências Ambientais - UNESP, Campus Sorocaba (SP), e-mail: miqueiaseng@hotmail.com (autor correspondente); [2]Prof Dr do Programa de Pós-Graduação em Geografia – UNIR, Porto Velho (RO), e-mail: eliomar@unir.br; [3]Prof Dr. do Instituto de Educação Agricultura e Ambiente – IEAA/UFAM, Humaitá (AM), e-mail: hescosta@ufam.edu.br; [4]Doutoranda em Ciências Ambientais - UNESP, Campus Sorocaba (SP), e-mail: tatiana.acacio@unesp.br

Artigo recebido em 12/08/2020 e aceito em 02/08/2021

A B S T R A C T

The spread of deforestation in the Amazon region is a cause for concern, seeing as the breakdown of soil-forest equilibrium provokes and possibly accelerates several processes, including superficial erosion. This process is one of the major causes of soil degradation worldwide. The Revised Universal Soil Loss Equation (RUSLE) is a well-established and widely applied indirect method used to estimate soil loss, generating information that helps the conservation and proper management of soil and subsiding the policies of land use and occupation. This study estimated the potential of loss by laminar erosion of soil in the area of the basin of the Juma river, located in the municipality of Apuí, in the Southern Amazonas State. The RUSLE method was used to estimate soil loss in conjunction with GIS techniques. The results showed a predominance of areas with a high Natural Potential (NP) for erosion (200 to 600 $t.ha^{-1}.y^{-1}$), occupying about 77.58% of the examined region, and indicated that this high index is related to the LS factor. In relation to Soil Loss (SL), it was observed that there is a predominance of small potential (0 to 10 $t.ha^{-1}.y^{-1}$), occurring in 72.96% of the area, and the highest indices of soil loss (> 120 $t.ha^{-1}.y^{-1}$) were observed only in places occupied by exposed soil or farming areas where there are no conservation practices associated with terrain slope in place, which reiterates the importance of the adoption of appropriate agricultural practices.

Keywords: Soil loss, RUSLE, Juma watershed, Brazilian Amazon.

Avaliação da Erosão do Solo Usando o Modelo RUSLE e SIG na bacia hidrográfica do rio Juma, no Sul do Estado do Amazonas

R E S U M O

O aumento do desmatamento na Amazônia é motivo de preocupação, visto que com a quebra do equilíbrio solo-floresta provoca o aceleramento de vários impactos, incluindo a erosão superficial do solo. Esse processo é uma das principais causas de degradação do solo em todo o mundo. A Equação Universal de Perda de Solo (RUSLE) é um método indireto bem estabelecido e amplamente utilizado para estimar a perda do solo, gerando informações que ajudam na conservação e manejo adequado do solo e subsidiando as políticas de uso e ocupação. Este estudo estimou o potencial de perda por erosão laminar do solo na bacia do rio Juma, localizada no município de Apuí, no Sul do Estado do Amazonas. O método RUSLE foi utilizado para estimar a perda de solo em conjunto com as técnicas de SIG. Os resultados mostraram a predominância de áreas com alto Potencial Natural (PN) de erosão (200 a 600 $t.ha^{-1}.ano^{-1}$), ocupando cerca de 77,58% da região avaliada, indicando que esse alto índice está relacionado ao fator LS. Em relação à Perda de Solo (PS), observou-se que há predominância de pequeno potencial (0 a 10 $t.ha^{-1}.ano^{-1}$), ocorrendo em 72,96% da área, e os maiores índices de perda de solo (> 120 $t.ha^{-1}.ano^{-1}$) foram observados apenas em locais ocupados por solo exposto ou áreas agrícolas com ausência de práticas de conservação associadas à inclinação acentuada do terreno, o que reitera a importância da adoção de práticas agrícolas adequadas.

Palavras-chave: Perda de Solo, RUSLE, Bacia do Rio Juma, Amazônia Brasileira.

Introduction

Soil erosion is a natural geological process that shapes the landscape through the breakdown, transport and sedimentation of the particles that form the superficial layer that covers parts of the Earth's crust (Rangel et al., 2019; Pereira e Cabral, 2021). When it occurs expeditiously, this process can result in the loss of soil capacity to sustain plant

production. Nowadays, particularly due to the dependence that mankind has on agricultural production to meet its material needs for survival, the loss of the productive capacity of soil cannot be neglected, as it is almost a matter of survival. In Brazil, the concern with this degradation process is greater with Amazonian soils that are undergoing removal of their natural cover for agricultural use (Duarte et al., 2019; Reis et al., 2021).

In recent decades, the Amazon Region has been affected by a series of environmental impacts, mainly due to deforestation and fires associated with the process of expanding agricultural boundaries and increasing timber exploitation and prospection (Duarte et al., 2020; Mataveli et al., 2021).

Despite the impressive immensity of the Amazon region, the fragility of this system is also noteworthy. As already highlighted in several studies on the performance of vegetation cover in the protection of soils in the Amazon (Flores e Holmgren, 2021; Reis et al., 2021), if the breakdown of soil-vegetation equilibrium occurs, an increase in intense erosion processes can be observed, along with the compaction and impoverishment of soils (Duarte et al., 2020), consequently leading to the abandonment of unproductive areas (Silva et al., 2021), which contributes to increasing pressure to open new areas (Duarte et al., 2020).

Soil erosion may lead to the disablement of agricultural areas, soil compaction, removal of nutrients from the superficial layer and the siltation of water bodies. Rangel et al. (2019) and Duarte et al. (2020) call attention to both inappropriate use and occupation and the lack of conservation practices as some of the main factors responsible for soil erosion.

In the search for measures to combat erosion damage, several methods of assessing environmental impacts and soil loss have been widely used as tools in agro-environmental planning. In recent decades, several models of soil erosion measurement have been developed. Among them, we highlight the Revised Universal Soil Loss Equation, RUSLE, which has presented consistent results (Benavidez et al., 2018; Vansan e Tomazoni, 2020; Pereira e Cabral, 2021).

RUSLE is a simple model for predicting the laminar erosion of soils based on the integration between climatic, pedological, topographic and land use dynamics integrated in the Geographic Information System (GIS) environment. Due to its simplicity and the availability of input data, the RUSLE model is still the most widely used to estimate the average annual loss of soil over large areas, with acceptable accuracy (Kayet et al., 2018; Vansan e Tomazoni, 2020).

The municipality of Apuí, in the Southern Amazonas State, located in a strategic region between the state of Pará and Rondônia (known as the "Deforestation Arc"), has undergone considerable loss of natural vegetation coverage due to the expansion of agricultural and livestock activity (Sathler et al., 2018). According to data from the National Food Supply Company, CONAB in Portuguese (Brazil, 2017), in the last harvest, the municipality presented itself as a major exponent in the production of grains of the state of Amazonas. However, there is insufficient information regarding the susceptibility of soils in this region to erosion.

Due to the lack of information on soil loss that may occur in the region as a result of the removal of natural forest cover, this work was developed with the general objective of contributing to the gathering of information regarding the potential for soil loss by erosion of Amazonian soils, estimating and mapping the Natural Potential (NP) and Soil Loss (SL) in a laminar way with the application of the quantitative model RUSLE in the Juma watershed, in the municipality of Apuí located in the southern region of the state of Amazonas.

Materials and methods

Study area

The study area is located in the municipality of Apuí, in the Southern Amazonas State, under geographic coordinates 7°3'41.85" at 7°26'46.49" South and 59°54'6.55" at 60°12'41.47" West (Figure 1). Located in the 5th Sub-Region of the Madeira River, the municipality of Apuí is limited to the municipalities of Novo Aripuanã, Borba, Maués, Manicoré and the state of Mato Grosso (MT).

The municipality of Apuí emerged from the largest agricultural settlement project in South America (Juma river Settlement Project, Decree n° 238/1982), during the military government (Leal, 2009). The BR 230 (Transamazonian highway), which connects the municipality of Humaitá-AM (about 397 km, SW) and the municipality of Taraoacanga-PA (about 300 km away), is the main access road and outlet of production in the municipality.

According to Köppen climatic classification, the climatic characteristics in the municipality of Apuí are hot and humid, with a low-pronounced dry season, of the type "Am". The

average annual temperature varies between 25 and 27 °C, with averages of 26.3 °C, and the relative humidity is established at 85%, with the level of precipitation above 2,200 mm.y-1. The rainiest period in the Apuí region corresponds to the quarter from January to March and the least rainy season (drier period) is from July to August. The lowest temperatures occur in the months of June and July, with absolute minimums of 10 to 16 °C (Alvares et al., 2013).

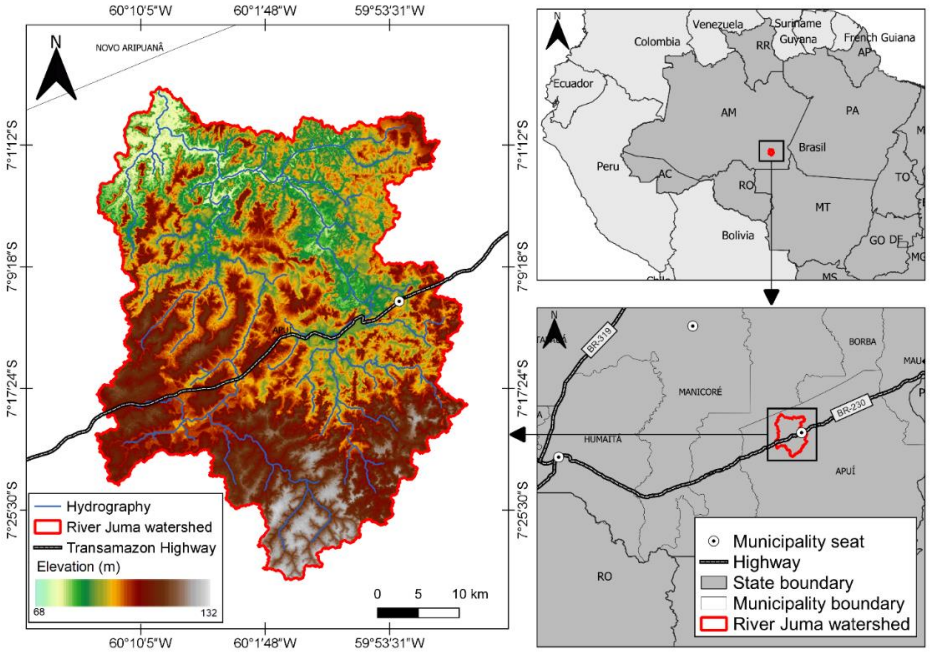

Figure 1. Location of the Juma River Watershed.

Revised Universal Soil Loss Equation-RUSLE

We chose the Revised Universal Soil Loss Equation-RUSLE for the ease of acquisition of input data, mainly in remote regions of difficult access as in the Amazon region. Although the USLE has well-known weaknesses, it is still the only model that allows medium and large size areas to be easily evaluated (Benavidez et al., 2018; Devátý et al., 2019).

The results of the soil loss estimates obtained in this study were compared to soil loss data obtained through field experiments conducted in the Amazon region, in order to verify the consistency of soil loss estimation performed by the method RUSLE.

Estimation of Annual Soil Loss

As proposed by Wischmeier and Smith (1978), in the model of the Universal Soil Loss Equation-USLE, the annual soil loss in tonnes per hectare is expressed by Equation 1.

$$A = R * K * L * S * C * P \quad (1)$$

Where A corresponds to the Soil Loss ($t.ha^{-1}.y^{-1}$); R = Rainfall erosivity ($MJ.mm.ha^{-1}.h^{-1}.y^{-1}$); K = Soil erodibility ($t.ha.h.ha^{-1}.MJ^{-1}.mm^{-1}$); L*S topographic factor (dimensionless); C = soil cover and management (dimensionless) and P = Conservationist practices (dimensionless).

Modifications have been proposed in some terms of the USLE to better approximate the estimates to the data in experimental plots. In this work, we adopted the Revised Universal Soil Loss Equation-RUSLE based on the USLE model proposed by Wischmeier and Smith (1978), which was developed by a group of scientists in the United States and soil conservationists that have had experiences with erosive processes (Benavidez et al., 2018; USDA, 2018).

In order to observe the effects of vegetation cover dynamics on soil loss rates in the study area more objectively, the Natural Potential (NP) of soil loss was obtained from the multiplication of natural factors (R*K*L*S), The NP, when presented in a cartographic form, allows a clear interpretation of the risk of erosion in a hydrographic basin depending on the natural characteristics of the physical environment (Durães e Mello, 2016; Morais e Sales, 2017).

Data Acquisition and Processing

The acquisition of spatial information for the application of the RUSLE method was based on access to public domain databases deposited in international, federal, state and municipal bodies,

as well as soil sampling in field for information validation. The cartographic products were made using QGIS software (version 3.2.3 "Bonn") with the Mercator/UTM Universal Transversa Coordinate reference system, and the reference base SIRGAS 2000, zone 20S.

R factor determination

Rainfall erosivity was obtained by applying the method proposed by Oliveira JR and Medina (1990), developed for the Manaus/AM Region (Equation 2).

$$R = 3.76 * \left(\frac{M_x^2}{A}\right) + 42.77 \quad (2)$$

Where M_x corresponds to the average monthly precipitation (mm); and A corresponds to the average annual rainfall (mm). Due to the low density of pluvimetric stations for the region, the R factor was determined from monthly precipitation data obtained through the radar sensor Tropical Rainfall Measuring Mission (TRMM). The data was obtained from the website of the National Aeronautics and Space Administration/NASA (NASA, 2018) with an observation period of 18 years (1998-2016). This data set relates to the 3b42-V7 product made available in GeoTiff format with spatial resolution of 0.25°X 0.25° (Nastos et al., 2016). Almeida et al. (2015) evaluated this product for the Amazonas State and concluded that the data of the TRMM satellite can contribute to rainfall studies in the region.

The data, covering18 years of precipitation, was grouped, the average monthly values were calculated, then the equation proposed by Oliveira JR and Medina was applied (1990), obtaining the average annual erosivity, which was interpolated by the Inverse Distance Weighting/IDW method. The average monthly precipitation and erosivity values were transformed into relative percentages and presented in chart form.

K factor determination

Soil erodibility was determined by the Denardin (1990) method, which proposed an adaptation to the monogram of Wischmeier et al. (1978) for the calculation of global erodibility. The calculations were performed using Equation 3.

$$K = 0.0000748M + 0.00448059P - 0.0631175DMP + 0.01039567R \quad (3)$$

Where:

K = global soil erodibility of Denardin (1990), $t.ha.h.ha^{-1}.MJ^{-1}.mm^{-1}$;

M = {(fine sand + silt) x [(fine sand + Silt) + coarse sand]}, %;

P = codified permeability according to Galindo and Margolis (1989);

DMP = {[(0.65 x coarse sand) + (0.15 x fine sand) + (0.0117 x silt) + (0.00024 x clay)]/100}, mm;

R = [sand – very fine sand x (%MO/100)].

Based on the Brazilian Soil Classification System – SiBCS (EMBRAPA, 2018), using the soil map provided by EMBRAPA/PA (EMBRAPA, 2018), scale 1:100,000 (Vila Apuí Articulation), 8 soil categories were identified in the area of study. However, soil samples were randomly sampled only in the larger orders (Argisols, Latosols and Spodosols). The definition of the sample number was based on the percentage of spatial occurrence of the suborders within each order.

The 10 sampling points of the Argisol order were distributed among the following identified suborders: (four of the Red Argisol class, five of the Yellow Argisol class, and one of the Red-Yellow Argisol class). The 10 sample points for the Latosol order were distributed as follows among the suborders: (three in the Yellow Latosol class, three in the Red Latosol class, and four in the Red-Yellow Latosol class). Another 10 points were distributed in the area of occurrence of the suborder Humuvic Spodosol, and one point for the Haplic Gleysol class.

Soil samples were taken from February 19th to 23rd, 2018. For each sampling point, a deformed sample was collected in the form of a lump, from the superficial layer (0-20 cm), and was subsequently dried and defuncted to obtain the TFSA (Dried Fine Soil in Open Air), according to the methodology described by EMBRAPA (1997).

The TFSA samples were subjected to physical (granulometric) and chemical (organic matter) analysis in the EMBRAPA-Rondônia Soil Laboratory. The granulometric analysis was performed by the pipette method, using a 1.0 mol L^{-1} NaOH solution as a chemical dispersing, with a resting time of 16 hours, as according to EMBRAPA (1997) methodology, which is used here to obtain the fractions of sand, silt and clay.

The particle size distribution of the sand fraction was determined by means of a sieve shaker, model SOLOTEST. Each sample of sand fraction from each soil sample was shaken for 3 minutes using the common sieves with meshes of 2mm; 1mm; 0.5mm; 0.250mm; 0.125mm and 0.053mm.

Organic Matter (OM) was estimated based on the organic carbon (CO) analysis according to Walkley-Black methodology, modified by Yeomans and Bremner (1988), based on the

premise that the hummus contains approximately 58% of carbon. Thus, the MO was estimated by Equation 4

$$MO = CO \times 1.724 \quad (4)$$

Where CO corresponds to the soil organic carbon obtained in the analysis.

The soil structure was determined directly in the field, defined by the dimensions of the structural element classes, based on the classes established in the Technical Handbook of Pedology (IBGE, 2007), and codified in the following classes: (i) very small granular = 1; (ii) small granular = 2; (iii) medium to large granular = 3 and (iv) blocks, laminar or massive = 4.

The permeability was determined according to the texture and degree of soil structure and codified based on the following classes: (i) fast = 1; (ii) moderate to rapid = 2; (iii) moderate = 3; (iv) slow to moderate; and (v) slow = 5, according to the method proposed by Galindo and Margolis (1989).

LS factor determination

The topographic factor was obtained by the methodology formulated by Desmet and Glover (1996), as presented in Equation 5. The LS factor tool is available in the TerrainAnalysis module of SAGA GIS (toolbox available in QGIS).

$$LSi,j = \frac{[(A_{i,j-in}+D^2)^{m+1}]}{[D^{m+2} * X_{i,j}^{m} * (22{,}13^{m})]} \quad (5)$$

Where, $A_{i,j-in}$ corresponds to the area of contribution of the cell with coordinated (i, j) (m^2); D corresponds to the size of the cell (m); m corresponds to the slope function coefficient for the cell grid with coordinates (i, j), where the coefficient (m) is obtained from the slope classes. The coefficient m=0.5, if the slope is > 5%; m=0, for the range of 3 to 5%; m=0.3 for the range of 1 to 3%; and m=0.2 for slope less than 1%. The variable X corresponds to the function of the spectrum for the coordinate cell grid (i, j), which can be obtained by the equation $X = \sin\alpha / \cos\alpha$ where alpha corresponds to the direction of flow in the strand. To obtain the LS factor, we used a Digital Model of Hydrologically Consistent Elevation (MDEHC) generated from mission data of the shuttle Radar Topography Mission/SRTM, available on the website of the United States Geological Survey-USGS (USGS, 2018), achieved joints S07_W060; S07_W061; S08_W060 and S08_W061, with original spatial resolution of 1 second arch (30 meters).

CP factor determination

The CP parameter was obtained by means of supervised classification of orbital images of the Sentinel-2 remote sensor, 20MRT and 20MRS articulation, passage date 05/08/2016, obtained from the USGS website (USGS, 2018).

The supervised classification was performed using the Semi-Automatic Classification Plugin tool (6.2.4 version. "Greenbelt") in QGIS, based on the spectral signature of the ROI (Regions of Interest) samples. The Maximum Likelihood (MaxVer) algorithm uses the data set from the pixel collection employed for the training of the map classes and creates a normal probability distribution of the values of all bands for each class (Duarte and Silva, 2019). Then, the classification was validated by calculating the Accuracy and Kappa index.

From the identification of the classes of soil use and occupation, the weights of the C Factor were attributed as observed in the literature. As for the P Factor, which refers to the adoption of conservation practices, the value attributed was 1 for the whole area, since the absence of a conservationist practice was observed. Table 1 shows the values adopted for the C Factor, as observed in literature for the six classes of land use and occupation observed in the area

.

Table 1. Factor C values observed in the literature.

Land use classes	C Factor	Source
Water	0.00	Farinasso et al. (2006) and Paes et al. (2010)
Exposed soil	1.00	Farinasso et al. (2006) and Paes et al. (2010)
Farming	1.00	Farinasso et al. (2006) and Paes et al. (2010)
Conserved Pasture	0.055	Vale Júnior et al. (2010) and Paes et al. (2010)
Degraded pasture	0.10	Paes et al. (2010) and Benavidez et al. (2018)
Forest	< 0.0004	Fernandes (2008) and Panagos et al. (2015)

Results

Erodibility of Rain Factor (R)

The monthly erosivity values observed for the study area for the considered period (18 years) ranged from 47.74 $MJ.mm.ha^{-1}.h^{-1}.y^{-1}$ to 145.73

MJ.mm.ha^{-1}.h^{-1}.y^{-1}, with an annual average of 1,300.67 (156.07±SD) MJ.mm.ha^{-1}.h^{-1}.y^{-1} for a total annual precipitation of 2,350.03 mm. These values were close to those observed by Oliveira JR and Medina (1990) for the Manaus/AM region, where an average annual rainfall of 2,355.6 mm.y^{-1} with erosivity of 1,177.55 MJ.mm.ha^{-1}.h^{-1}.y^{-1} was observed. According to Duarte and Silva Filho (2019), these values can be classified as low erosivity.

It was observed that the percentage values of monthly average erosivity in the study area increased according to the volume of precipitation in January, February, March and April. The erosivity expressed in percentage terms (R%) was higher than the relative percentage precipitation, suggesting that rainfall in these months was of greater erosive power, as shown in Figure 2. This same behavior was observed by Oliveira JR and Medina (1990).

In the months from July to December, there is an inversion, when the percentage values of erosivity do not exceed the percentage values of precipitation or become inferior. This behavior can be explained by the difference in rainfall intensities that occur distinctly in the two periods, that is, in the months from January to May, rainfall events are scattered and intense (Junior et al., 2018), thus increasing erosive power, as observed by Duarte and Silva Filho (2019).

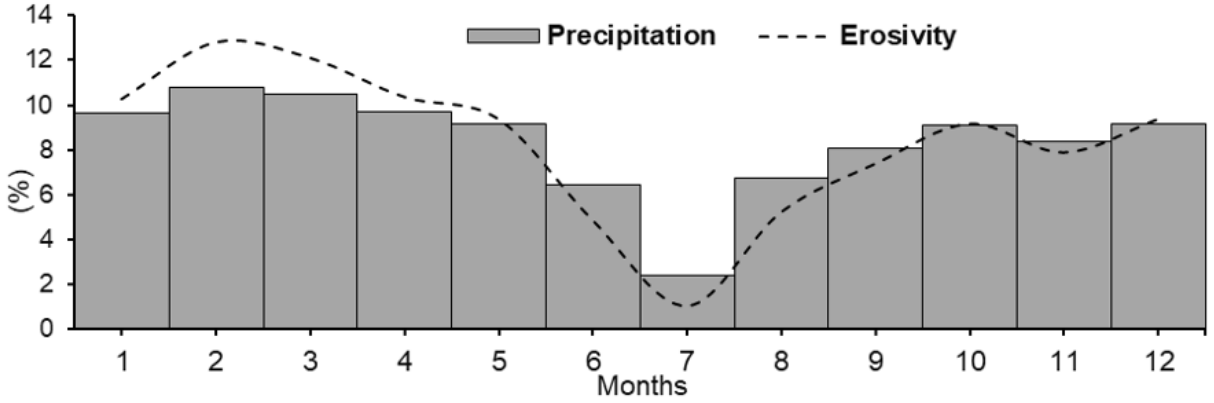

Figure 2. Monthly percentage distribution of rainfall and rainfall erosivity between 1998 and 2016.

Soil Erodibility Factor (K)

Table 2 presents the mean values of texture, organic matter and other parameters used for the application of Denardin (1990) methodology. It also presents the erodibility index for each soil unit observed in the and Soil Loss (SL) in a laminar way with the application of the quantitative model RUSLE in the Juma watershed.

Table 2. Erodibility values and parameters used in the Denardin (1990) equation to characterize the potential for erosion losses of the predominant soil orders of the Juma watershed.

Soil classes	Particles	MO (±SD)	M (±SD)	Permeability	DMP (±SD)	R (±SD)	K
Esg2	Weak sand	0.363 ± 0.031	736.45 ± 15.49	Moderate	0.558 ± 0.56	0.00765 ± 0.0017	0.036
GXdb2	Silt	0.143 ± 0.017	1,347.00 ± 128.29	Moderate	0.293 ± 0.095	0.02722 ± 0.0011	0.096
PAd8	Clay	0.455 ± 0.039	96.47 ± 7.54	Slow	0.061 ± 0.041	0.01047 ± 0.0010	0.029
PVd1	Clay	0.429 ± 0.041	350.3 ± 16.70	Fast	0.243 ± 0.018	0.00859 ± 0.00046	0.028
PVAd11	Clay	0.363 ± 0.032	60.96 ± 4.79	Moderate	0.041 ± 0.037	0.00436 ± 0.00039	0.015
LAd14	Clay	0.430 ± 0.045	196.82 ± 8.32	Slow	0.106 ± 0.010	0.00535 ± 0.00038	0.031
LVd11	Clay	0.447 ± 0.043	202.84 ± 5.60	Slow/Moderate	0.105 ± 0.013	0.00042 ± 0.00001	0.026
LVAd4	Clay	0.428 ± 0.040	361.39 ± 41.37	Slow/Moderate	0.251 ± 0.019	0.00858 ± 0.00001	0.031

Esg2 - Spodosols; GXdb2 - Gleysol; PAd8 - Yellow Argisol; PVd1 - Red Argisol; PVAd11 – Red-Yellow Argisol; LAD14 - Yellow Latosol; LVD11- Red Latosol; LVAD4 – Red-Yellow Latosol; M - Organic Matter; M - Indices of the Denardin equation; DMP: average particle diameter; K - Soil erodibility Index, expressed in t.ha.h.ha^{-1}.MJ^{-1}.mm^{-1}.

The erodibility values (K), among the soil units, ranged from 0.015 t.ha.h.ha^{-1}.MJ^{-1}.mm^{-1} to 0.096 t.ha.h.ha^{-1}.MJ^{-1}.mm^{-1}, being 0.031, 0.028, 0.096 and 0.036 t.ha.h.ha^{-1}.MJ^{-1}.mm^{-1} for the classes of Latosols, Argisols, Gleysols and Spodosols respectively.

High values (0.096 t.ha.h.ha^{-1}.MJ^{-1}.mm^{-1}) were observed for the Gleysol class. These indices may be related to the high contents of the sand fraction that directly interfere in the determination of K factor, as observed by Demarchi and Zimback (2014). The erodibility observed in the other soil classes showed values close to those observed in other regions of Brazil (Mannigel et al., 2002; Cassol et al., 2018), and in studies with Amazonian soils (Silva et al., 2018; Gato et al., 2018).

According to the classification defined by Mannigel et al. (2002), the study area presents 50.63% with low erodibility, followed by 27.48%; 18.04% and 3.82% with moderate, very low and high erodibility of the soil.

Topographic Factor (LS)

The study area presents a predominantly wavy (45.36%) to gently wavy slope (33.44%), and only 11.76% corresponds to heavily wavy and mountainous terrain, and finally 9.35% to flat areas. The largest soil class corresponds to the Red Argisol (38.06%), and class is distributed under predominantly wavy terrain (45.76%) to gently wavy (33.81%), followed by heavily wavy (10.72%) and 9.54% of flat land, respectively. The other soil classes also present similar distributions.

Table 3 presents the classes of the LS factor obtained by the method of Desmet and Govers (1996), from which it is observed that classes 2-3 and 3-4 correspond to 89% of the study area, while the classes of higher erosive potential (6-7 and 7-8) occupy about 0.81% of the total area. This result indicates that in the region a low potential for soil loss predominates due to rain laminar erosion.

Table 3. Class frequency of the LS factor in the Juma watershed.

Declivity (%)	LS factor classes	Area (km²)	Area (%)
0 to 3	0-1	0.18	0.01
0 to 3	1-2	1.91	0.10
3 to 8	2-3	996.80	55.00
3 to 8/8 to 20	3-4	612.15	34.00
8 to 20	4-5	143.90	7.90
8 to 20	5-6	50.03	2.70
20 to 45	6-7	14.43	0.80
45 to 75	7-8	1.21	0.1

CP factor

The classification supervised by the MaxVer method presented an accuracy of 80.44% and a Kappa index of 0.66, which, according to the classification described by Duarte and Silva (2019), is considered as very good. Table 4 shows the distribution of the classes of land use and occupation in the area.

The sites occupied by soil exposed in the study area pedominantly concur with areas where short-cycle agricultural activities are concentrated, such as maize, rice and bean plantations, common activities in the region, as observed in the field. In such places, soil concentrations in the vicinity of the roads were also observed, and areas of degraded pasture or areas of recent burn, all in dimensions not detected due to the low spatial resolution of the images used. The agricultural areas in turn are occupied predominantly by long cycle activities such as coffee, cacoa, cupuaçu and banana plantations.

The areas identified as pasture correspond to the places occupied by cattle-raising activities in good cultivation conditions and suitable rotating and grazing practices, while the other areas identified as degraded pasture correspond to the areas that are under disordered use due to supergrazing, showing characteristics of degraded areas.

The areas occupied by dense forest represent the class of soil with greater scope in the basin of the Juma river (60.04%), together with the areas occupied by dispersed forest with 12.69% representing 72.73% of the total. These areas exert natural protection in the soil against the action of laminar erosion by reducing the impact of raindrops and the volume of the runoff, in addition to allowing higher infiltration rates.

However, in the last 16 years, the areas occupied by pasture have increased significantly in function, especially, of the increment of bovine flock, which was higher between 2002 and 2004, when the herd more than doubled. The increase of the bovine herd drives the need to open new areas for the establishment of pasture, as described by Duarte et al. (2019).

Table 4. Distribution of the class of land use and occupation in the Juma watershed obtained from the supervised classification.

Land use Classes	Factor CP	Area (km²)	Area (%)
Water	0.0	1.96	0.10
Exposed soil	1.0	14.42	0.80
Agriculture	1.0	3.16	0.17
Degraded Pasture	0.1	245.13	13.61
Conserved Pasture	0.055	226.03	12.55
Dispersed Forest	0.0004	228.51	12.69
Dense Forest	0.0004	1,080.78	60.04

Legend: Factor CP: Value attributed to the type of land use classes.

Spatial Distribution of R, K, LS and CP Factors

Figure 3 shows the spatial distribution of R (a), K (b), LS (c) and CP (d) factors for the study area. With regard to the R factor (Figure 3a), it was found that there is greater erosivity in the northern region of the watershed, while the smallest indices are distributed in small portions in the southern and eastern region of the Juma watershed, that is, the mean erosivity increases from the source to the mouth. It is noteworthy that the spatial variation of the rainfall erosivity index along the Juma watershed is small (average of 11.66 MJ.mm. $ha^{-1}.h^{-1}.y^{-1}$), the greatest variations are related to regional seasonality.

In relation to the K factor (Figure 3b), its spatial distribution in the study area is analogous to the distribution of pedological classes, thus distributed in percentage terms: Red Argisol (38.06%); Red-Yellow Argisol (18.05%); Yellow Argisol (16.60%); Spodosol (8.29%); Yellow Latosol (8.05%); Red Latosol (4.29%); Gleysols (3.83%) and Red-Yellow Latosol (2.84%).

The spatial distribution of the LS factor is arranged in Figure 3c, in which it is observed that the highest values are near the hilltops and along the water bodies. This occurs as a function of the method, which provides, pixel by pixel, the value of LS along the strands. In addition, it uses the concept of accumulated flow of upstream drainage, thus, when the values of the source flow are high, the method tends to also estimate high values of the LS factor, especially in the positions close to the drainage (Desmet and Govers, 1996).

Figure 3d presents the spatial distribution of the CP factor, in which the greater scope of the class occupied by dense and dispersed forests that make up about 72.73% of the area is observed, adding natural protection against superficial erosion. On the other hand, only 0.80% of the area is occupied by exposed soil, which corresponds to the soil use class of greater susceptibility to erosion because it is in direct contact with the action of rain. As was also observed in Figure 3d, the spatial distribution of the different classes of coverage, the predominance of forest coincident with the ciliary area and springs suggests that there is cause for conservationist concern.

Natural Potential and Soil **Loss**

Table 5 presents the Natural Potential (NP) and Soil Loss (SL) classes for the study area.

Table 5. NP and SL class in the Juma watershed.

Natural Potential for Soil Loss ($t.ha^{-1}.year^{-1}$)		
Classes	**Area (km²)**	**Area (%)**
0 to 100 (Weak)	2.30	0.13
100 to 200 (Average)	26.39	1.47
200 to 600 (High)	1,396.60	77.58
600 to 1,000 (Very high)	369.72	20.54
>1,000 (Extremely high)	4.99	0.28
Soil Loss ($t.ha^{-1}.year^{-1}$)		
0 to 10 (Small)	1,313.33	72.96
10 to 15 (Moderate)	6.95	0.38
15 to 50 (Average)	354.97	19.74
50 to 120 (Strong)	106.87	5.93
>120 (Very strong)	17.88	0.99

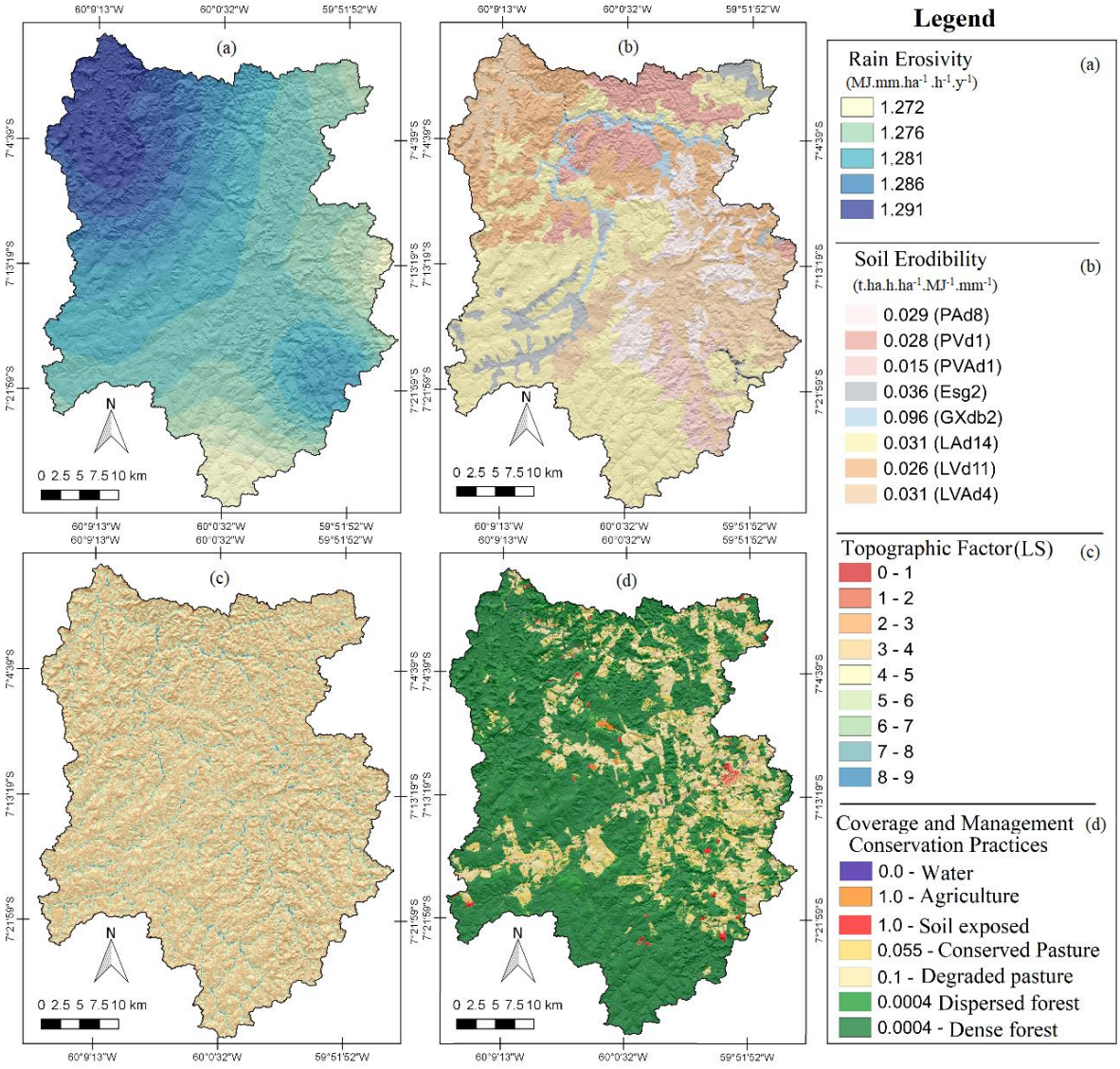

Figure 3. Spatial distribution of R (a), K (b), LS (c) and CP (d) factors for the study area.

The class that presented high NP and SL (200 to 600 t.ha^{-1}.y^{-1}) occupies about 77.58% of the study area, followed by the very high class (1,600 to 3,200 t.ha^{-1}.y^{-1}) representing about 20.54%, and extremely high (> 1,000 t.ha^{-1}.y^{-1}) with about 0.28%, totaling 98.4% of the Juma watershed. On the other hand, the class identified as moderate (100 to 200 t. ha^{-1}.y^{-1}) and weak natural potential (0 to 100 t.ha^{-1}.y^{-1}) makes up only 1.6% of the area, that is, the Juma watershed presents a high natural potential for soil loss due to the high rates of rainfall associated with terrain and soil characteristics.

On the other hand, when the soil loss is analyzed, there is a predominance of a small potential for laminar erosion (0 to 10 t.ha^{-1}.y^{-1}) covering about 73.96% of the area. These sites are occupied by natural vegetation that protects against intense erosive processes. The areas occupied by exposed soil or by agricultural activity with the absence of conservation practices and adequate management systems have a very strong loss class (above 120 t. ha^{-1}.y^{-1}), occupying approximately 0.99% of the area.

It was observed that the natural potential of soil erosion has a strong influence of LS factor, and to a lesser extent, the K factor. The percentage distribution of the loss potential classes in the area represented in Figure 4a evidences the strong association between the NP and the LS factor classes for the study area. This result points to the importance of the aspect of the terrain, which, in turn, presents the wavy form in the majority. The contribution of this factor in the NP of local soil erosion evidences the importance of adopting conservationist practices and adequate management systems in order to avoid the advancement of erosive processes at the site.

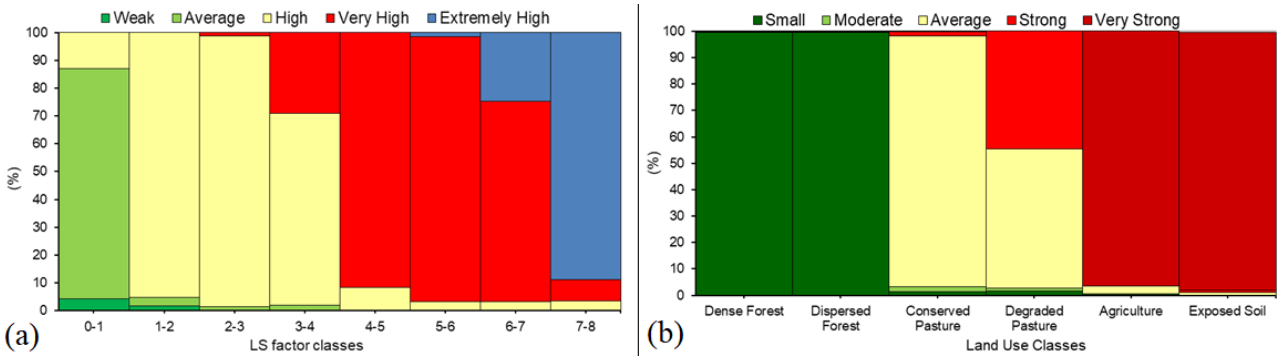

Figure 4. Relative percentage between NP of soil loss with Factor LS (a), and SL with land use and occupation (b).

Figure 5a presents the spatial distribution of the NP and SL for the study area. Regarding the NP, the strong association with the spatial distribution of the LS factor is observed, and to a lesser extent, of the K factor, in which the occurrences of high potential soil loss classes happen mainly along the slopes and top of hills, characteristics observed in the spatial distribution of the LS factor. An association with the K factor is also observed, albeit in smaller proportions, the latter can be easily noticed in the portions that have medium NP, analogous areas to the sites constituted by the class of Spodosols, with erodibility equal to 0.036 $t.ha^{-1}.y^{-1}$.

As for SL (Figure 5b), there was a strong association between the classes of soil loss with their classes of use and occupation. This relationship can be noted from the comparison between the use and occupation (Figure 3d) of the soil and the SL (Figure 5b). The relative percentage distribution presented (Figure 4b) clearly shows this relationship (reinforced by the overlap between use and occupation with the spatial distribution of the potential for losses). In summary, the sites that have a small potential for SL are predominantly occupied by forests, while the areas occupied by the classes that have very strong erosion potential, in general, correspond to the exposed soil class.

The spatial distribution of NP and SL in the study area shows two possible scenarios (Figure 5). The first shows that most of the areas with marked topography are covered by natural vegetation, and the second shows the little spatial coverage of the exposed soil class, which corresponds to the higher risk of SL in the area.

Discussion

Table 6 shows a comparison between the results obtained by the RUSLE method and those observed in a field experiment in the Amazon region. In general, the RUSLE method has a strong tendency to underestimate soil loss in the study area, by up to 38.40%.

Table 6. Comparison between soil loss by direct and indirect method.

Method	Forest	Dispersed Forest	Pasture	Exposed soil
	----------Soil Loss ($t.ha^{-1}.y^{-1}$)----------			
Experiment	11.15*	18.54***	35.8**	286.07**
RUSLE (±SD)	3.10 ± 2.31	12.89 ± 1.66	31.48 ± 12.99	169.12 ± 25.00

*Machado (2010), **Arruda et al., (2004), ***Encinas (2011).

According to Benavidez et al. (2018), this underestimation can occur due to the fact that the method only takes only soil loss through sheet and rill erosion into account, disregarding erosion on margins, erosion in the river canal and landslides. Schmidt et al. (2019) and Barrena-González et al. (2020) mention that this underestimation may be related to the scale of the area, because the method tends to overestimate on a small scale and underestimate on a large scale.

In preserved forest area, the RUSLE method estimated average losses of 3.10 $t.ha^{-1}.y^{-1}$, and in field experiments, Machado (2010) observed losses of 11.15 $t.ha^{-1}.y^{-1}$. Both values are well higher than the global average values, which are 0.004 to 0.05 $t.ha^{-1}.y^{-1}$ (Benavidez et al., 2018). The high rates of soil loss observed in the forest area can be justified by local conditions (high precipitation rates, sandy soil texture) that strongly influence the loss of soil in the region (Machado, 2010; Encinas, 2011; Duarte et al., 2019; Duarte et al., 2020).

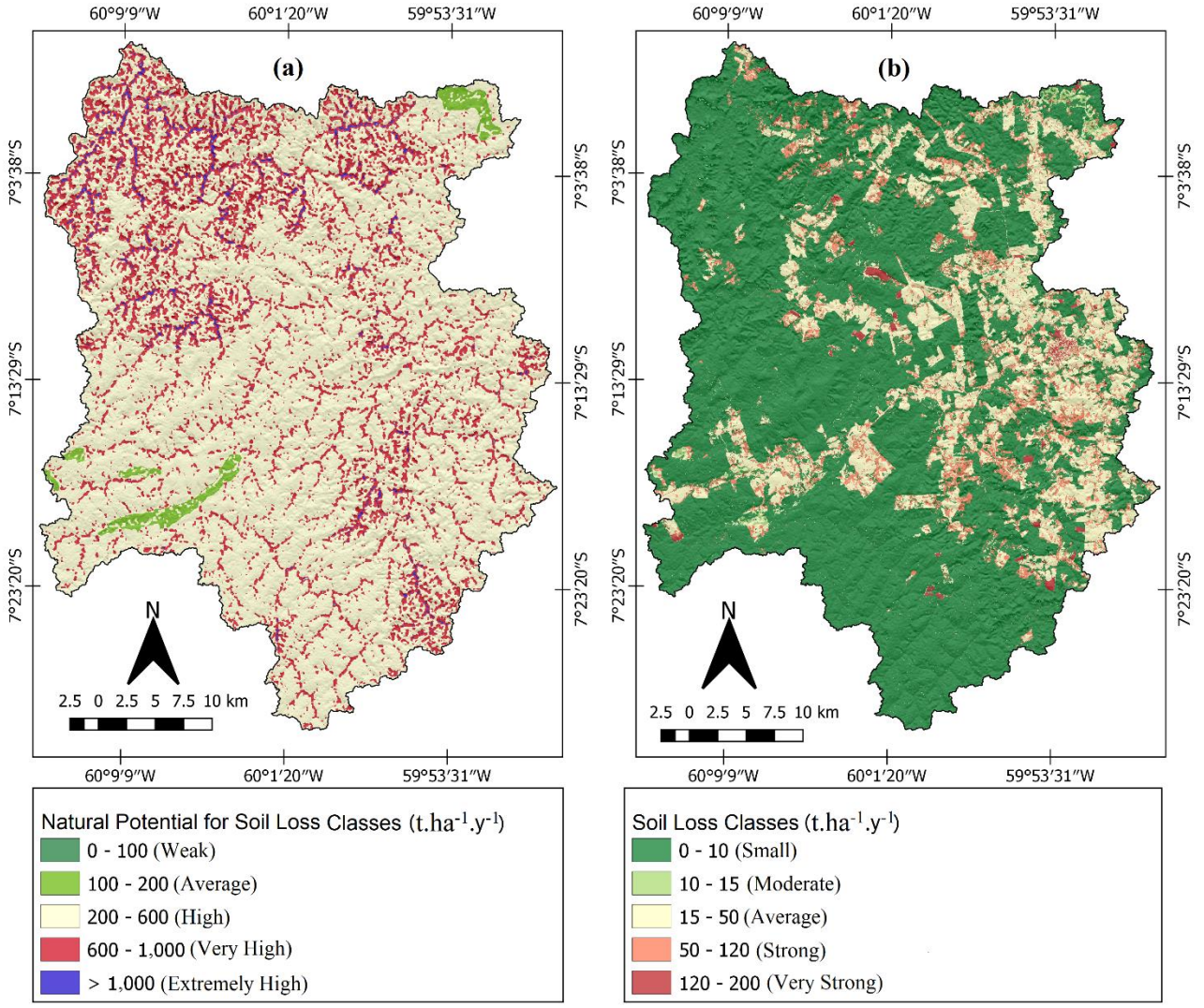

Figure 5. NP (A) and SL (B) map for the Juma watershed.

The average soil losses estimated for the plant regeneration class were 12.89 $t.ha^{-1}.y^{-1}$, while in field experiment the mean values were 18.54 $t.ha^{-1}.y^{-1}$. In the pasture-occupied areas, the estimated soil losses were 31.45 $t.ha^{-1}.y^{-1}$ and those observed in experiments were 35.8 $t.ha^{-1}.y^{-1}$. The areas occupied by exposed soil presented higher potential for estimated soil loss (169.12 $t.ha^{-1}.y^{-1}$), as was also observed in the field (286.07 $t.ha^{-1}.y^{-1}$). This area together with pasture has percentages of soil loss above the values admitted by the Food and Agriculture Organization of the United Nations - FAO (FAO, 2015). However, the adoption of appropriate cultivation practices can considerably reduce soil loss (Encinas, 2011; Duarte et al., 2020).

Comparing the maps of NP (Figure 5a) and SL (Figure 5b), the importance exerted by the natural vegetation cover of the soil through the decrease of the superficial erosion is verified. If, on the one hand, the NP does not take into account the vegetation cover, soil loss occurs with greater intensity and in larger areas due to the lack of natural protection. On the other hand, when considering the natural or anthropic protection factor related to the vegetation cover, the erosion index decreases considerably, approaching zero. In other words, vegetation cover associated with adequate agricultural practices contributes strongly to the maintenance of low rates of average annual soil losses (Panagos et al., 2015; Sampaio et al., 2016).

The values of the percentage of spatial occurrence of exposed soil (0.8% - Table 4), when compared to the percentage of spatial occurrence of the very strong loss class (0.99% - Table 5) reinforce the importance of the vegetation coverage in the prevention of soil losses for this region, as described by several studies (Labrière et al., 2015; Duarte et al., 2019). Considering the current dynamics of land use in the Amazon (EMBRAPA, 2016), the need to implement effective

environmental public policies aimed at minimizing the exposure of these areas becomes evident. The effect of itinerant farming (Ferreira et al., 2018; Barlow et al., 2019) and supergrazing practices that are common in the Amazon region can accelerate the loss of soil in large scales.

Conclusions

Evaluation of soil loss in the Juma watershed using the RUSLE method in a GIS environment has highlighted the areas most exposed to erosion. The methodology used proved to be satisfactory and can be considered an alternative for regions with insufficient precise data, such as the Amazon region.

Comparing the maps of Natural Potential and Soil Loss reinforces the importance exerted by natural vegetation cover by decreasing losses due to superficial erosion. The high potential classes of soil loss occupy about 77.58% of the area, with potential losses between 200 to 600 $t.ha^{-1}.y^{-1}$, followed by 20.54% of the area classified as very high natural potential, where losses are between 600 to 1,000 $t.ha^{-1}.y^{-1}$, demonstrating the region's high vulnerability to soil degradation.

With the presence of vegetation cover, the loss scenario is significantly altered. The areas in which high potential predominates (200 to 600 $t.ha^{-1}.y^{-1}$) show low losses (soil losses lower than 10 $t.ha^{-1}.y^{-1}$), and, in some areas, this index approaches zero, which demonstrates the adequacy of the analysis model adopted here.

As an encouragement, we observed that the sites where higher soil losses occurred, especially in discovered areas and agricultural areas with no conservation practices associated with steep slope, can be controlled with the adoption of appropriate conservationist practices. This reinforces the importance of the use of soil in an adequate way to minimize losses by laminar erosion.

Acknowledgements

This work was supported by the National Council for Scientific and Technological Development, which grants a scholarship to the main author (grant number 145574/2016-4). The authors thank the Geoprocessing Laboratory of the Universidade Federal do Amazonas-IEAA-UFAM, for providing the space for the development of this research, and the Brazilian Agricultural Research Corporation (EMBRAPA, its acronym in Portuguese), especially Prof[a]. PhD Marília Locatelli (in memory) for guidance and soil analysis.

References

Almeida, C.T., Delgado, R.C., Junior, J.F.O., Gois, G., Cavalcanti, A.S., 2015. Avaliação das Estimativas de Precipitação do Produto 3B43-TRMM do Estado do Amazonas. Floresta e Ambiente 22, 279-286. http://dx.doi.org/10.1590/2179-8087.112114

Alvares, C.A., Stape, J.L., Sentelhas, P.C., Gonçalves, J.L.M., Sparovek, G., 2013. Köppen's climate classification map for Brazil. Meteorologische Zeitschrift 22, 711-728. http://dx.doi.org/10.1127/0941-2948/2013/0507

Arruda, W.C., Lima, H.N., Forsberg, B.R., Teixeira, W.G., 2004. Estimativa de erosão em clareiras através da mudança do relevo do solo por meio de pinos. In: 1° Wolrkshop Técnico-Científico da Rede CT-Preto Amazônia. Manaus. 4p.

Barlow, J., Berenguer, E., Carmenta, R., França, F., 2019. Clarifying Amazonia's burning crisis. Global Change Biology 26, 319-321. https://doi.org/10.1111/gcb.14872

Barrena-González, J., Rodrigo-Comino, J., Gyasi-Agyei, Fernández, M.P., Cerdà, A. 2020. Applying the RUSLE and ISUM in the Tierra de Barros Vineyards (Extremadura, Spain) to Estimate Soil Mobilisation Rates. Land 9, 1-17. https://doi.org/10.3390/land9030093

Benavidez, R., Jackson, B., Maxwell, D., Norton, K., 2018. A review of the (Revised) Universal Soil Loss Equation ((R)USLE): with a view to increasing its global applicability and improving soil loss estimates. Hydrology and Earth System Sciences 22, 6059–6086. https://doi.org/10.5194/hess-22-6059-2018

Cassol, E.A., Silva, T.S., Eltz, F.L.F., Levien, R. 2018. Soil Erodibility under Natural Rainfall Conditions as the K Factor of the Universal Soil Loss Equation and Application of the Nomograph for a Subtropical Ultisol. Revista Brasileira de Ciência do Solo 42, 1-12. https://doi.org/10.1590/18069657rbcs20170262

CONAB-Companhia Nacional de Abastecimento. 2017. Acompanhamento da safra brasileira de grão: safra 2016/2017. 1, 1-104.

Demarchi, J.C., Zimback, C.R.L., 2014. Mapeamento, erodibilidade e tolerância de perda de solo na sub-bacia do Ribeirão das Perobas. Revista Energia na Agricultura 29, 102-114. https://doi.org/10.17224/EnergAgric.2014v29n2p102-114

Denardin, J.E., 1990. Erodibilidade do solo estimada por meio de parâmetros físicos e químicos. Tese (Doutorado), Piracicaba, USP.

Desmet, P.J.J.J., Govers, G. 1996. A GIS-Procedure for Automatically Calculating the USLE LS-Factor on Topographically Complex Landscape Units. Journal of Soil and Water Conservation 51, 427-433.

Devátý, J., Dostál, T., Hösl, R., Krása, J., Strauss, P., 2019. Effects of historical land use and land pattern changes on soil erosion – Case studies from Lower Austria and Central Bohemia. Land Use Policy 82, 674-685. https://doi.org/10.1016/j.landusepol.2018.11.058

Duarte, M.L., Brito, W.B., Silva, T.A., Castro, A. L. Padrões e causas do desmatamento no Baixo Acre, região oeste da Amazônia brasileira. Journal of EnvironmentalAnalysis and Progress. v. 5, n.1. p. 117-127. 2020. https://doi.org/10.24221/jeap.5.1.2020.2790.117-127

Duarte, M.L., Silva Filho, E.P., 2019. Estimation of rain erosion in the Juma river basin based on TRMM satellite data. Caderno de Geografia 29, 45-60. https://doi.org/10.5752/P.2318-2962.2019v29n56p45

Duarte, M.L., Silva Filho, E.P., Brito, W.B.M., Silva, T.A., 2020. Determinação da erodibilidade do solo por meio de dois métodos indiretos em uma bacia hidrográfica na região sul do estado do Amazonas, Brasil. Revista Brasileira de Geomorfologia 21, 329-341. http://dx.doi.org/10.20502/rbg.v21i2.1533

Duarte, M.L., Silva, T.A., 2019. Avaliação do desempenho de três algoritmos na classificação de uso do solo a partir de geotecnologias gratuitas. Revista de Estudos Ambientais 21, 6-16. http://dx.doi.org/10.7867/1983-1501.2019v21n1p6-16

Duarte, M.L., Silva, T.A., Cerqueira, C., Silva Filho, E.P., 2019. Pressões Ambientais em Unidades de Conservação: estudo de caso no sul do Estado do Amazonas. Revista de Geografia e Ordenamento do Território 18, 108-125. http://dx.doi.org/10.17127/got/2019.18.005

Durães, M.F., Mello, C.R., 2016. Distribuição espacial da erosão potencial e atual do solo na Bacia Hidrográfica do Rio Sapucaí, MG. Engenharia Sanitária e Ambiental 21, 677-685. https://doi.org/10.1590/s1413-41522016121182

EMBRAPA - Centro Nacional de Pesquisa de Solos (CNPS). 1997. Manual de métodos de análise de solo. EMBRAPA. Rio de Janeiro. 2ª Ed. 1-211.

EMBRAPA - Empresa Brasileira de Pesquisa Agropecuária. 2018. MAPA de solos da área piloto de Apuí - Amazonas: folha: Vila Apuí.

EMBRAPA - Empresa Brasileira de Pesquisa Agropecuária. 2018. Sistema brasileiro de classificação de solos. Embrapa, 5. ed. E-book. Brasília.

Encinas, O.C., 2011. Avaliação de processos erosivos na base de operações geólogo Pedro de Moura - Coari, AM. Dissertação (Mestrado), Manaus, INPA.

FAO - Food and Agriculture Organization. 2015. Status of the World's Soil Resources (SWSR) – Technical Summary. Food and Agriculture Organization of the United Nations and Intergovernmental Technical Panel on Soils, Rome, Italy. 95p.

Farinasso, M., Júnior, O.A.C., Guimarães, R.F., Gomes, R.A.T., Ramos, V.M., 2006. Avaliação Qualitativa do Potencial de Erosão Laminar Em Grandes Áreas Por Meio da EUPS – Equação Universal de Perdas de Solos Utilizando Novas Metodologias Em SIG Para os Cálculos dos Seus Fatores na Região do Alto Parnaíba – PI-MA. Revista Brasileira de Geomorfologia 7, 73-85.

Fernandes, L. C., 2008. Estudo multi-temporal do uso, ocupação e perda de solos em projetos de assentamento em Rondônia. Tese (Doutorado), Rio Claro, UNESP.

Ferreira, M.P.S., Artur, A.G., Queiroz, H.M., Romero, R.E., Costa, M.C.G., 2018. Changes in attributes of soils subjected to fallow in desertification hotspot. Revista Ciência Agronômica 49, 22-31. http://dx.doi.org/10.5935/1806-6690.20180003

Flores, B., Holmgren, M. White-Sand Savannas Expand at the Core of the Amazon After Forest Wildfires, Ecosystems. 2021. https://doi.org/10.1007/s10021-021-00607-x

Galindo, I.C., Margolis, E., 1989. Tolerância de perdas por erosão para solos do Estado de Pernambuco. Revista Brasileira Ciência do Solo 13, 95-100.

Gato, L.C., Costa, H.S., Duarte, M.L., 2018. Erodibility of soils in southern Amazonas State for two Indirect Methods. In: 21 WORLD CONGRESS OF SOIL SCIENCE.

IBGE – Instituto Brasileiro de Geografia e Estatística. 2007. Manual Técnico de Pedologia. 2 Ed. Rio de Janeiro, RJ - Brasil. 316p.

Junior, A.L.P., Querino, C.A.S., Querino, J.K.A.S., Santos, L.O.F., Moura, A.R.M., Machado, N.G., Biudes, M.S., 2018. Variabilidade horária e intensidade sazonal da precipitação no município de Humaitá-AM. Revista brasileira de Climatologia 22, 463-475. http://dx.doi.org/10.5380/abclima.v22i0.58089

Kayet, N., Pathak, K., Chakrabarty, A., Sahoo, S., 2018. Evaluation of soil loss estimation using the RUSLE model and SCS-CN method in hillslope mining areas. International Soil and Water Conservation Research 6, 31-42. https://doi.org/10.1016/j.iswcr.2017.11.002

Labrière, L., Locatelli, B., Laumonier, Y., Freycon, V., Bernoux, M., 2015. Soil erosion in the humid tropics: A systematic quantitative review. Agriculture, Ecosystems & Environment 203, 127-139. https://doi.org/10.1016/j.agee.2015.01.027

Leal, P.F., 2009. Colonização agrícola dirigida e construção de parceleiros tutelados. Antropolítica 2, 155-182. https://doi.org/10.22409/antropolitica2009.2i27.a9

Machado, F.S., 2010. Erosão hídrica sob chuva simulada em diferentes classes de solos e coberturas vegetais na província petrolífera de Urucu – Coari, AM. Dissertação (Mestrado), Manaus, UFAM.

Mannigel, A.R., Carvalho, M.P., Moreti, D., Medeiros, L.R., 2002. Fator erodibilidade e tolerância de perda dos solos do Estado de São Paulo. Acta Scientiarum Agronomy 24, 1335-1340. http://dx.doi.org/10.4025/actasciagron.v24i0.2374

Mataveli, G.A.V., Chaves, M.E.D,. Brunsel, N.A., Aragão, L.E.O.C. The emergence of a new deforestation hotspot in Amazonia. Perspectives in Ecology and Conservation. v. 19, n. 1, p. 33-36. 2021. https://doi.org/10.1016/j.pecon.2021.01.002

Morais, R.C.S., Sales, M.C.L., 2017. Estimativa do Potencial Natural de Erosão dos Solos da Bacia Hidrográfica do Alto Gurguéia, Piauí-Brasil, com uso de Sistema de Informação Geográfica. Caderno de Geografia 27, 84-105. https://doi.org/10.5752/p.2318-2962.2017v27nesp1p84

NASA - Data Tropical Rainfall Measuring Mission. Available in: https://giovanni.gsfc.nasa.gov/giovanni, Accessed: 01 December 2018.

Nastos, P.T., Kapsomenakis, J., Philandras, K.M., 2016. Evaluation of the TRMM 3B43 gridded precipitation estimates over Greece. Atmospheric Research 169, 497-514. https://doi.org/10.1016/j.atmosres.2015.08.008

Oliveira Jr.R.C., Medina, B.F., 1990. A erosividade das chuvas em Manaus (AM). Revista Brasileira Ciência do Solo 14, 235-239.

Paes, F.S., Dupas, F.A., Silva, F.G.B., Pereira, J.C.D., 2010. Espacialização da perda de solo nas bacias hidrográficas que compõem o município de Santa Rita do Sapucaí (MG). Geociências 29, 589-601.

Panagos, P., Borrelli, P., Meusburger, K., Alewell, C., Lugato, E., Montanarella, L., 2015. Estimating the soil erosion cover-management factor at the European scale. Land Use Policy 48, 38-50. http://dx.doi.org/10.1016/j.landusepol.2015.05.021

Pereira, M. D. R.; Cabral, J. B. P. Perda de solo no alto curso das bacias hidrográficas dos ribeirões Taquaruçu Grande e Taquaruçuzinho, Palmas (TO). Revista Brasileira de Geografia Física. v. 14, n.1. p. 332-339, 2021. http://dx.doi.org/10.26848/rbgf.v14.1.p332-339

Rangel, L., Jorge, M. C., Guerra, A., Fullen, M., 2019. Soil Erosion and Land Degradation on Trail Systems in Mountainous Areas: Two Case Studies from South-East Brazil. Soil systems 3, 1-14. https://doi.org/10.3390/soilsystems3030056

Reis, M., Graça, P. M.L.A., Yanai, A.M., Ramos, C.J.P, Fearnside, P.M. Forest fires and deforestation in the central Amazon: Effects of landscape and climate on spatial and temporal dynamics. Journal of Environmental Management, v. 288, 2021. https://doi.org/10.1016/j.jenvman.2021.112310

Sampaio, A.C.P., Cordeiro, A.M.N., Bastos, F.H., 2016. Susceptibilidade à erosão relacionada ao escoamento superficial na sub-bacia do Alto Mundaú, Ceará, Brasil. Revista Brasileira de Geografia Física 9, 125-143. https://doi.org/10.26848/rbgf.v9.1.p125-143

Sathler, D., Adamo, S.B., Lima, E.E.C., 2018. Deforestation and local sustainable development in Brazilian Legal Amazonia: an exploratory analysis. Ecology and Society 23, 1-15. https://doi.org/10.5751/ES-10062-230230

Schmidt, S., Alewell, C., Meusburger, K., 2019. Monthly RUSLE soil erosion risk of Swiss grasslands. Journal of Maps 15, 247-256. https://doi.org/10.1080/17445647.2019.1585980

Silva, A.S., Duarte, M.L., Costa, H.S., 2018. Erodibility of a Yellow Latosol (LA) under pasture and SAF in the southern region of Amazonas, Brazil by two Indirect Methods. In: 21 WORLD CONGRESS OF SOIL SCIENCE.

Silva, R.O., Barioni, L.G., Moran, D. Fire, deforestation, and livestock: When the smoke clears. Land Use Policy, v. 100. 2021.https://doi.org/10.1016/j.landusepol.2020.104949

USDA - United States Department of Agriculture. 2018. Revised Universal Soil Loss Equation (RUSLE) - Welcome to RUSLE 1 and RUSLE 2. Available in: https://www.ars.usda.gov Accessed: 26 November 2019.

USGS. 2018. Shuttle Radar Topography Mission (SRTM) 1 Arc-Second Global. Available at (Accessed in 11 December 2018). Available in: https://earthexplorer.usgs.gov/ Accessed: 26 November 2019

Vale Júnior, J.F., Barros, L.S., Sousa, M.I.L., Uchoa, S.C.P., 2009. Erodibilidade e suscetibilidade à erosão dos solos de cerrado com plantio de Acacia Mangium em Roraima. Agro@mbiente On-line 3, 1-8. http://dx.doi.org/10.18227/1982-8470ragro.v3i1.253

Vansan, A.P., Tomazoni, J.C. Uso de Técnicas de Geoprocessamento para Estudo da Erosão Hídrica Laminar em Microbacia Hidrográfica do Sudoeste do Paraná. Revista Brasileira de Geografia Física v.13, n.3. p. 1117-1131. 2020. https://doi.org/10.26848/rbgf.v13.3.p1117-1131

Wischmeier, W.H., Smith, D.D., 1978. Predicting rainfall erosion losses: a guide to conservation planning. Agriculture and book, 537, Washington, DC: USDA.

Yeomans, J.C., Bremner, J.M., 1988. A rapid and precise method for routine determination of organic carbon in soil. Communications in Soil Science and Plant Analysis 19, 1467-1476.